J|A|C|S ARTICLES

Published on Web 04/14/2009

Charge Density Analysis of the (C−C)→Ti Agostic Interactions in a Titanacyclobutane Complex

Stephan Scheins,[†] Marc Messerschmidt,[†] Milan Gembicky,[†] Mateusz Pitak,[†] Anatoliy Volkov,[‡] Philip Coppens,*[,†] Benjamin G. Harvey,[§] Gregory C. Turpin,[§] Atta M. Arif,[§] and Richard D. Ernst*[,§]

Department of Chemistry, University of New York at Buffalo, Buffalo, New York 14260, Department of Chemistry, Middle Tennessee State University, Mufreesboro, Tennessee 37132, and Department of Chemistry, University of Utah, Salt Lake City, Utah 84112

Received October 1, 2008; E-mail: coppens@buffalo.edu (P.C.); ernst@chem.utah.edu (R.D.E.)

Abstract: The experimental electron density study of $Ti(C_5H_4Me)_2[(CH_2)_2CMe_2]$ provides direct evidence for the presence of (C−C)→Ti agostic interactions. In accord with the model of Scherer and McGrady, the $C_\alpha-C_\beta$ bond densities no longer show cylindrical symmetry in the vicinity of the Ti atom and differ markedly from those of the other C−C bonds. At the points along the $C_\alpha-C_\beta$ bond where the deviation is maximal the electron density is elongated toward the metal center. The distortion is supported by parallel theoretical calculations. A calculation on an Mo complex in which the agostic interaction is absent supports the Scherer and McGrady criterion for agostic interactions. Despite the formal d^0 electron configuration for this Ti(IV) species, a significant nonzero population is observed for the d orbitals, the d orbital population is largest for the d_{xy} orbital, the lobes of which point toward the two C_α atoms. Of the three different basis sets for the Ti atom used in theoretical calculations with the B3LYP functional, only the 6-311++G** set for Ti agrees well with the experimental charge density distribution in the $Ti-(C_\alpha-C_\beta)_2$ plane.

1. Introduction

The first claim of a compound having a C−C single bond coordinated to a metal appeared in 1955.[1] The purported (cyclopropane)Pt complex was subsequently shown to have undergone (reversible) oxidative addition, yielding a metallacyclobutane.[2] Although the generally weak nature of M−C bonds and the highly directional nature of C−C bonds should substantially disfavor (C−C)→M agostic interactions relative to their common C−H and H−H analogues,[3−8] an early indication that (C−C)→M interactions could exist in isolable species was provided from a theoretical study by Morokuma et al. in which a (C−C)→M interaction was modeled using a known (C−Si)→M complex.[9] Indeed, the first confirmed examples of (C−C)→M agostic coordination were reported shortly afterward, in 1998,[10] the species having been isolated from pentadienyl/alkyne coupling reactions. Their nature was demonstrated by a combination of structural, theoretical, and spectroscopic data, particularly $^{13}C-^{13}C$ coupling constants derived primarily through NMR studies. Subsequently, a number of other examples have been reported, some again resulting from alkyne coupling reactions.[11−13] Interesting examples have even been discovered containing agostic interactions involving a C−C bond in a cyclopropyl ring, just as had originally been proposed in the platinum complex above,[14−16] as well as in some "σ-arenium" rhodium complexes.[17−19]

Although (C−C)→M agostic interactions are of interest in their own right, and are of clear importance for C−C bond activations,[20] other studies have suggested that these interactions could play a role in the olefin polymerization and metathesis

[†] University at Buffalo.
[‡] Middle Tennessee State University.
[§] University of Utah.

(1) Tipper, C. F. H. *J. Chem. Soc.* **1955**, 2045.
(2) Adams, D. M.; Chatt, J.; Guy, R. G.; Sheppard, N. J. *J. Chem. Soc.* **1961**, 738–742.
(3) Low, J. J.; Goddard, W. A. I. *J. Am. Chem. Soc.* **1984**, *106*, 8321–8322.
(4) Blomberg, M. R. A.; Siegbahn, P. E. M.; Nagashima, U.; Wennerberg, J. *J. Am. Chem. Soc.* **1991**, *113*, 424–433.
(5) Siegbahn, P. E. M.; Blomberg, M. R. A. *J. Am. Chem. Soc.* **1992**, *114*, 10548–10556.
(6) Rybtchinski, B.; Oevers, S.; Montag, M.; Vigalok, A.; Rozenberg, H.; Martin, J. M. L.; Milstein, D. *J. Am. Chem. Soc.* **2001**, *123*, 9064–9077.
(7) Hinrichs, R. Z.; Schroden, J. J.; Davis, H. F. *J. Am. Chem. Soc.* **2003**, *125*, 860–861.
(8) Crabtree, R. H.; Holt, E. M.; Lavin, M.; Morehouse, S. M. *Inorg. Chem.* **1985**, *24* (13), 1986–1992.
(9) Koga, N.; Morokuma, K. *J. Am. Chem. Soc.* **1988**, *110*, 108–112.
(10) Tomaszewski, R.; Hyla-Kryspin, I.; Mayne, C. L.; Arif, A. M.; Gleiter, R.; Ernst, R. D. *J. Am. Chem. Soc.* **1998**, *120*, 2959–2960.
(11) Rosenthal, U.; Pellny, P.-M.; Kirchbauer, F. G.; Burlakov, V. V. *Acc. Chem. Res.* **2000**, *33*, 119–129.
(12) Harvey, B. G.; Arif, A. M.; Ernst, R. D. *J. Organomet. Chem.* **2006**, *691*, 5211–5217.
(13) Harvey, B. G.; Arif, A. M.; Ernst, R. D. *J. Mol. Struct.* **2008**, *890*, 107–111.
(14) Jaffart, J.; Etienne, M.; Reinhold, M.; McGrady, J. E.; Maseras, F. *J. Chem. Soc., Chem. Commun.* **2003**, 876–877.
(15) Goldfuss, B.; Schleyer, P. v. R.; Hampel, F. *J. Am. Chem. Soc.* **1996**, *118*, 12183–12189.
(16) Brayshaw, S. K.; Sceats, E. L.; Green, J. C.; Weller, A. S. *Proc. Natl. Acad. Sci. U.S.A.* **2007**, *104*, 6921–6926.
(17) Gandelman, M.; Shimon, L. J. W.; Milstein, D. *Chem.—Eur. J.* **2003**, *9*, 4295–4300.
(18) van der Boom, M. E.; Milstein, D. *Chem. Rev.* **2003**, *103*, 1759–1792.
(19) Frech, C. M.; Milstein, D. *J. Am. Chem. Soc.* **2006**, *128*, 12434–12435.

 10.1021/ja807649k CCC: $40.75

reactions, as well as in cyclopropanation[21] and deinsertion reactions.[22,23] In the first case, this could involve termination steps,[24−32] while in the latter, a (C−C)→M agostic interaction could promote the reversion of a metallacyclobutane to the free olefin and a metal carbene complex. Indeed, theoretical, spectroscopic, and structural data have recently confirmed the presence of (C−C)→M agostic interactions in electron-deficient metallacyclobutanes.[12,31−36] Additionally, a structural database search has revealed other metallacyclobutanes that appear to possess (C−C)→M interactions,[33] and structural and spectroscopic comparisons with early, electron deficient metallacyclobutadienes have led to the proposal that these species also contain (C−C)→M agostic interactions.[13] However, each of the methods used for establishing these agostic interactions suffers limitations. Solution-phase NMR spectroscopy can be ineffective in cases involving paramagnetic, poorly soluble, or thermally unstable compounds. Likewise, there can be problems in unambiguously assessing the data from routine structural studies, as the C−C bond lengthening in agostic complexes can be quite modest and even unobservable.[10,12,13,32] Further, it has been shown that a close contact between an electron-deficient metal center and a given bond does not necessarily lead to an agostic interaction.[37] Hence, there is a need to expand upon the methods through which the presence of agostic interactions, especially those involving C−C bonds, may be assessed.

Careful electron density studies through low-temperature X-ray diffraction can provide very useful information not accessible by other techniques, as they can be applied to paramagnetic, thermally sensitive, and insoluble compounds. In particular, an examination of electron density can ideally be used to ascertain whether a close contact between atoms actually corresponds to a bonding interaction or not. We have reported such a study on a zirconium pentadienyl complex in which a close Zr···C−H contact exists.[38] The bond ellipticity profile criterion recently proposed by Scherer and McGrady[39] is particularly valuable in the case of metal···C−C interactions in which the ambiguity resulting from the low scattering power of the H atom does not exist. In this contribution we apply the electron density approach to an example of an electron deficient titanacyclobutane already established to contain a (C−C)→Ti agostic interaction,[32] and verify the ability of electron density methods to assess the presence of C−C agostic interactions.

In the choice of an appropriate complex for study, titanacyclobutanes having no β-hydrogen atoms were desired, in order to avoid competitive (C−H)→M agostic interactions.[4] $Ti(C_5H_4Me)_2[(CH_2)_2CMe_2]$ is a suitable choice, as it crystallizes in a centrosymmetric space group ($C2/c$). A routine structural study indicated its suitability for a more careful electron density study.

The crystal structures of related compounds have been determined previously.[40−42] The main features of the title complex are elongated C−C bonds in the coordinated neopentadiyl ligand. The neighboring bonds to the coordinated carbon atom have a length of 1.575(1) Å compared to the other two C−C single bonds in the same ligand of 1.536(4) Å, the latter having a standard single bond length. This elongation can be explained within the concept of an agostic interaction and is the first indicator of an activated C−C bond. A detailed charge density analysis is presented in this paper to further shed light on the bonding situation in this special bond. This analysis is based on the aspherical-atom multipole refinement of the high-resolution X-ray data using the XD program package.[43] Values from theoretical calculations at the experimental geometry are presented for comparison purposes.

2. Experimental Section

$Ti(C_5H_4Me)_2[(CH_2)_2C(Me)_2]$ was prepared by a modification of a previously reported procedure.[44] $Ti(C_5H_4Me)_2CH_2AlMe_2Cl$ (0.50 g) was dissolved in ca. 4 mL of toluene in a 250 mL three-neck flask equipped with a dry ice condenser, a nitrogen inlet, and a stir bar. The flask was cooled to −30 °C, and ca. 5 mL of isobutylene was condensed into the flask. Finely powdered DMAP (4-dimethylaminopyridine, 0.21 g) was added, and the temperature of the flask was allowed to increase until the isobutylene refluxed slowly for 5 min. The flask was again cooled to −30 °C, and 25 mL of cold (−30 °C) pentane was added. The solution was swirled several times and then left to sit at this temperature for 30 min. The supernatant was then syringed away from the resulting polycrystalline orange solid and transferred to a Schlenk flask. The solvent was concentrated in vacuo at 0 °C to ca. 2 mL and the flask then placed in a −60 °C freezer overnight to yield a dark red mass of solid that was subsequently recrystallized from a minimal amount of toluene at −30 °C to give 0.24 g (54%) of deep red cubic crystals of the compound. More of the compound could be recovered from the concentrated supernatant, but it was somewhat oily. At room temperature, the crystalline solid slowly converts to

(20) Dzwiniel, T. L.; Stryker, J. M. *J. Am. Chem. Soc.* **2004**, *126*, 9184–9185.
(21) Rodriguez-Garcia, C.; Oliva, A.; Ortuno, R. M.; Branchadell, V. *J. Am. Chem. Soc.* **2001**, *123*, 6157–6163.
(22) Hill, G. S.; Puddephatt, R. J. *Organometallics* **1998**, *17*, 1478–1486.
(23) Ujaque, G.; Maseras, F.; Lledos, A.; Contreras, L.; Pizzano, A.; Rodewald, D.; Sanchez, L.; Carmona, E.; Monge, A.; Ruiz, C. *Organometallics* **1999**, *18*, 3294–3305.
(24) Eshius, J. J. W.; Tan, Y. Y.; Meetsma, A.; Teuben, J. H.; Renkema, J.; Evens, G. G. *Organometallics* **1992**, *11*, 362–369.
(25) Kawamura-Kuribayashi, H.; Koga, N.; Morokuma, K. *J. Am. Chem. Soc.* **1992**, *114*, 2359–2366.
(26) Yang, X.; Stern, C. L.; Marks, T. J. *J. Am. Chem. Soc.* **1994**, *116*, 10015–10031.
(27) Corker, J.; Lefebvre, F.; Lécuyer, C.; Dufaud, V.; Quignard, F.; Choplin, A.; Basset, J.-M. *Science* **1996**, *271*, 966–969.
(28) Resconi, L.; Piemontesi, F.; Franciscono, G.; Abis, L.; Fioriani, T. *J. Am. Chem. Soc.* **1992**, *114*, 1025–1032.
(29) Lanza, G.; Fragalà, I. L.; Marks, T. J. *J. Am. Chem. Soc.* **2000**, *122*, 12764–12777.
(30) Horton, A. D. *Organometallics* **1996**, *15*, 2675–2677.
(31) Suresh, C. H.; Koga, N. *Organometallics* **2004**, *23*, 76–80.
(32) Harvey, B. G.; Mayne, C. L.; Arif, A. M.; Tomaszewski, R.; Ernst, R. D. *J. Am. Chem. Soc.* **2005**, *127*, 16426–16435.
(33) Suresh, C. H.; Baik, M.-H. *J. Chem. Soc., Dalton Trans.* **2005**, 2982–2984.
(34) Suresh, C. H. *J. Organomet. Chem.* **2006**, *691*, 5366–5374.
(35) Lord, R. L.; Wang, H.; Vieweger, M.; Baik, M.-H. *J. Organomet. Chem.* **2006**, *691*, 5505–5512.
(36) Rowley, C. N.; van der Eide, E. F.; Piers, W. E.; Woo, T. K. *Organometallics* **2008**, *27*, 6043–6045.
(37) Maseras, F.; Crabtree, R. H. *Inorg. Chim. Acta* **2004**, *357*, 345–346.
(38) Pillet, S.; Wu, G.; Kulsomphob, V.; Harvey, B. G.; Ernst, R. D.; Coppens, P. *J. Am. Chem. Soc.* **2003**, *125*, 1937–1949.
(39) Scherer, W.; McGrady, G. S. *Angew. Chem., Int. Ed.* **2004**, *43*, 1782–1806.
(40) Lee, J. B.; Gajda, G. J.; Schaefer, W. P.; Howard, T. R.; Ikariya, T.; Straus, D. A.; Grubbs, R. H. *J. Am. Chem. Soc.* **1981**, *103*, 7358–7361.
(41) Greidanus, G.; McDonald, R.; Stryker, J. M. *Organometallics* **2001**, *20*, 2492–2504.
(42) Polse, J. L.; Kaplan, A. W.; Andersen, R. A.; Bergman, R. G. *J. Am. Chem. Soc.* **1998**, *120*, 6316–6328.
(43) Volkov, A.; Macchi, P.; Farrugia, L. J.; Gatti, C.; Mallinson, P. R.; Richter, T.; Koritsanszky, T. XD2006 - A computer program package for multipole refinement, topological analysis of charge densities, and evaluation of intermolecular energies from experimental and theoretical structure factors, 2006.
(44) Finch, W. C. A., E.V.; Grubbs, R.H. J. *J. Am. Chem. Soc.* **1988**, *110*, 2406–2413.

Table 1. Crystallographic Information

temperature [K]	90
space group	*C*2/*c*
volume [Å^3]	2907.1
Z	8
no. of reflns	93 347
unique reflns	12 643
completeness	99.8
redundancy	7.37
refln/param ratio	16.7
R(int)	2.53
R1(SHELX)[a]	2.28
R1(multi)[a]	1.13
$\Delta\rho$[e/Å^3]	0.199 −0.186
GOF	1.82

[a] Residual based on reflections with $I > 3\sigma(I)$.

a dark black-red oil; however, under an inert atmosphere at −30°, the crystals show no change after one month.

To investigate the charge density distribution of the title compound, a high resolution X-ray diffraction experiment at 90 K was performed using Mo Kα radiation from a rotating anode generator. Eleven different sets of data were collected, each covering a 180° ω range with a step size of 0.3°, four at a low 2θ setting of the detector with 8 s per frame, two at an intermediate range with a 15 s frame time, and three high-order runs with a 30 s exposure time per frame. The data were integrated with the APEXII software and merged with SORTAV,[45] which resulted in a maximum resolution of $(\sin\theta)/\lambda = 1.0$ Å^{-1}.

This allowed a full refinement of the aspherical density distribution according to the Hansen−Coppens formalism.[46] As a starting point of the refinement the independent atom model was used. The multipoles were introduced in a stepwise manner (first only monopoles, then additional dipoles, etc. until a full hexadecapole expansion was reached). The two 4s electrons of the Ti atom are not refined. They are very diffuse and contribute only to the scattering in the very low order region. For hydrogen atoms the multipole expansion was truncated at the dipole level. In the final stage the expansion parameters κ were refined for non hydrogen atoms, while the κ's for the hydrogen atoms were fixed at 1.2. The reflection-to-parameter ratio in the final refinement was 16.7. The refinement resulted in featureless residual density maps and converged with a final agreement factor of R1 = 1.1%. Further details are listed in Table 1.

3. Theoretical Calculations

For comparison purposes theoretical calculations at the experimental geometry were performed with Gausian03.[47] In all cases extensive 6-311++G** basis sets were used for the light atoms. To examine basis-set effects in the theoretical calculations three different basis sets were used for the Ti atom. They are the Dobbs and Hehre 6-311++G**,[48] the Wachters+f,[49] and the LANLDZ[50] basis sets. Calculations were done with both the B3LYP and the PBE1 functionals. As the results were essentially identical only the former are reported below. In order to compare the Ti compound with a metallacyclobutane ring compound with no agostic interaction, additional calculations were made on a Mo compound in which the metal/$C_\alpha-C_\beta$ agostic interaction is absent.[32] To compare the ellipticity along the bond path of the C−C bonds in the four-membered ring the same basis sets were selected for the Ti and Mo compounds (cc-pVTZ). For the visualization of the theoretical deformation densities, ellipticity and Laplacian maps the program DEN-PROP/WFN2PLOTS [51,52] was used. A full topological analysis was performed using the program Aimpac.[53] Calculations were performed on an in-house cluster consisting of 48 CPUs.

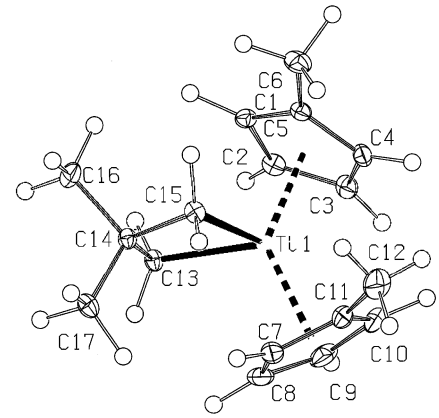

Figure 1. ORTEP representation with 50% probability ellipsoids

4. Results and Discussion

4.1. Molecular Structure. The geometry of the title compound is essentially identical to that of its C_5H_5 analogue published earlier,[40] except that standard deviations are lower in the current study. The molecular structure is displayed in Figure 1, together with the atomic numbering scheme. The Ti and three C atoms (C13, C14, and C15) of the neopentadiyl fragment form a nearly planar titanacyclobutane ring system, with the dihedral angle between the Ti−C15−C13 and C13−C14−C15 planes equaling only 6.7(1)°. As observed earlier, the most striking feature is the elongation of the C−C bonds in this four-membered-ring to 1.5723(3) and 1.5772(3) Å, compared with the conventional C−C single bond length of 1.54 Å. As described below this lengthening is accompanied by a significant distortion of the electron density in the two C−C bonds.

4.2. Topological Analysis of the Bonding and Comparison with Theoretical Values. Topological analysis of the charge density is an increasingly powerful tool for the characterization of bonding.[54,55] The experimental charge density at the bond-critical-points (BCPs) (shown in Figure 2) shows excellent transferability for all carbon−carbon bonds within each of the four different CC bond types in the complex (Table S1, column 4). The aromatic bonds of the Cp ligand have a much higher electron density (average 2.09(4) e/Å^3) at the BCP than the C−C single bonds in the neopentadiyl ligand. For the C−C single bonds the highest density at the BCP is found for the two Cp−Me bonds (1.81(2) e/Å^3), followed by the C14−CH_3 single bonds in the neopentadiyl ligand (1.64(2) e/Å^3), and the lowest value is found for the substantially elongated $C_\alpha-C_\beta$ (C13/C15−C14) bonds in the neopentadiyl ligand (1.50(2) e/Å^3). The values of the Laplacian, which agree reasonably well within

(45) Blessing, R. H. *J. Appl. Crystallogr.* **1997**, *30*, 421–426.
(46) Hansen, N. K.; Coppens, P. *Acta Crystallogr.* **1978**, *A34*, 909–921.
(47) Frisch, M. J. *Gaussian 03, Revision C.02*; Gaussian, Inc.: Wallingford, CT, 2004.
(48) Dobbs, K. D.; Hehre, W. J. *J. Comput. Chem.* **1986**, *7* (3), 359–378.
(49) Wachters, A. J. H. *J. Chem. Phys.* **1970**, *52* (3), 1033–1036.
(50) Hay, P. J.; Wadt, W. R. *J. Chem. Phys.* **1985**, *82* (1), 270–283.
(51) Volkov, A, Koritsansky, T., Chodkiewicz, M., King, H. F., J. Comput. Chem., in press
(52) Volkov, A. *Program WFN2PLOTS*; University at Buffalo, State University of New York: Buffalo, 2005.
(53) Cheeseman, J.; Keith, T. A.; Bader, R. F. W. *AIMPAC program package*; McMaster University: Hamilton, Ontario, 1992.
(54) Gatti, C. *Z. Kristallogr.* **2005**, *220*, 399–457.
(55) Koritsanszky, T. S.; Coppens, P. *Chem. Rev.* **2001**, *101*, 1583–1628.

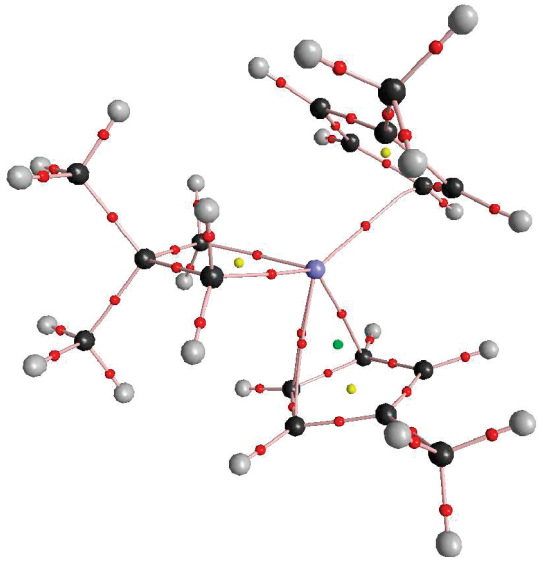

Figure 2. Molecular graph derived from the experimental density bond path (orange), BCPs (red), ring critical points (yellow), cage critical point (green).

each bond type, show the same trend. The most negative values are found for the aromatic bonds (−16.1(2) e/Å^5), whereas the two Cp−CH_3 bonds (−13.5(5) e/Å^5) have more negative values than the C−C bonds in the neopentadiyl ligand (average values of −10.6(1) and −8.3(1) e/Å^5 for C_β−CH_3 and the elongated C_α−C_β bonds, respectively).

The electron densities and the values of the Laplacians at the BCPs are compared with theoretical results in Table S1. The different theoretical calculations agree well for ρ_{BCP} and reasonably well for the values of the Laplacian. Similarly, the experimentally determined ρ_{BCP}'s agree well with theory, but the agreement is less good for the Laplacians, which are more negative for the light atom shared bonds, and much higher for the Ti−C_α bonds according to the experiment. It has been noted that the experimental values of $\nabla^2\rho$ are affected by the nature of the radial functions used in the aspherical atom refinement, but the difference for the Ti−C_α BCPs is larger than that found in other cases,[56] suggesting a genuine difference between theory and experiment. The result was confirmed in two additional experimental measurements of the charge density which gave identical results and are not reported here.

The experimental and theoretical deformation densities in the cyclopentadienyl ring agree well with each other (Figure 3a and b, only the theoretical Wachters result is shown, the others being essentially identical). But discrepancies in the Ti−C_α region are again evident. The Wachters+f and LanL2DZ calculations (Figure 4a and b) give much less pronounced bonding features than observed experimentally (Figure 4d), while the Dobbs and Hehre basis set (Figure 4c) is in much better agreement with experiment.

A corresponding section of the theoretical and experimental Laplacian is shown in Figure 4e and f, while a three-dimensional view is presented in Figure 4g and h. Both clearly show the charge concentration on the Ti atom in the direction of the C_α carbons. As is typical in strained four-membered ring systems, the density lobes at the C_α carbon atoms directed toward the Ti atoms are displaced outward from the internuclear vectors.[32] As expected, no such distortion is evident in the deformation densities of the five-membered cyclopentadienyl rings (Figure 3a and b).

A complete analysis of the topology reveals some differences between the two Cp ligands. While one of the ligands (Cp2, C7−C12) is connected to the Ti atom by three bond paths, for the other ring just one bond path connecting to the Ti is found. However, the difference corresponds to only very small differences in the electron density. As the density at the BCPs and the CCP (cage-critical point) of the Cp rings have almost the same value, small changes can result in the disappearance of a critical point. This point has recently been emphasized in a detailed study by Farrugia et al.[57]

Cremer and Kraka introduced the characterization of chemical bonding by analysis of the local energy densities at the bond critical points.[58] The theoretical kinetic energy density G(**r**) can be derived from the inner product of the gradients of the orbital electron densities ρi and their occupation numbers, ni. The potential energy density V(**r**) is related to $\nabla^2\rho$ and G(**r**) by the local virial theorem.[59] The total energy density, defined by (H(**r**) = G(**r**) + V(**r**)), is negative at the BCP for covalent bonds[58] for which the value of G(**r**) and the magnitude of V(**r**) increase. It is generally understood that for bonds between first row atoms the ratio G(**r**)/ρ(**r**) is less than unity for shared interactions and greater for closed-shell interactions.[54,59,60] Similarly, larger negative value of the ratio H(**r**)/ρ(**r**) indicates a more shared character of the interaction. However, Macchi and Sironi[60] and later Gibbs and co-workers[61] have recently shown that for bonds of both main group and transition metal atoms with oxygen the G(**r**)/ρ(**r**) ratio increases as the bond shortens and obtains more shared character.

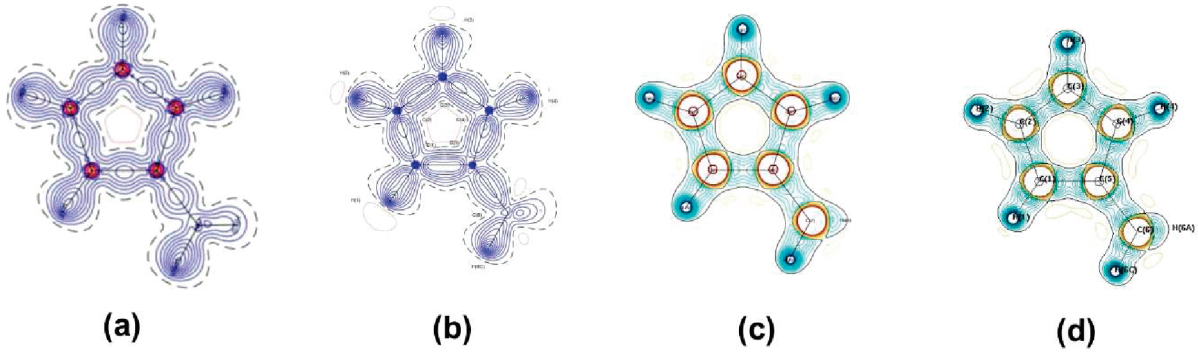

Figure 3. Deformation densities in the plane of a methylcyclopentadienyl ligand ((a) theory, Dobbs and Hehre; (b) experiment) contour interval 0.1 e/Å^3, blue/red: positive/negative (left/middle), and Laplacians contour ((c) theory, 6-311++G** for Ti atom; (d) experiment) interval 5 e/Å^5 blue/orange: negative/positive.

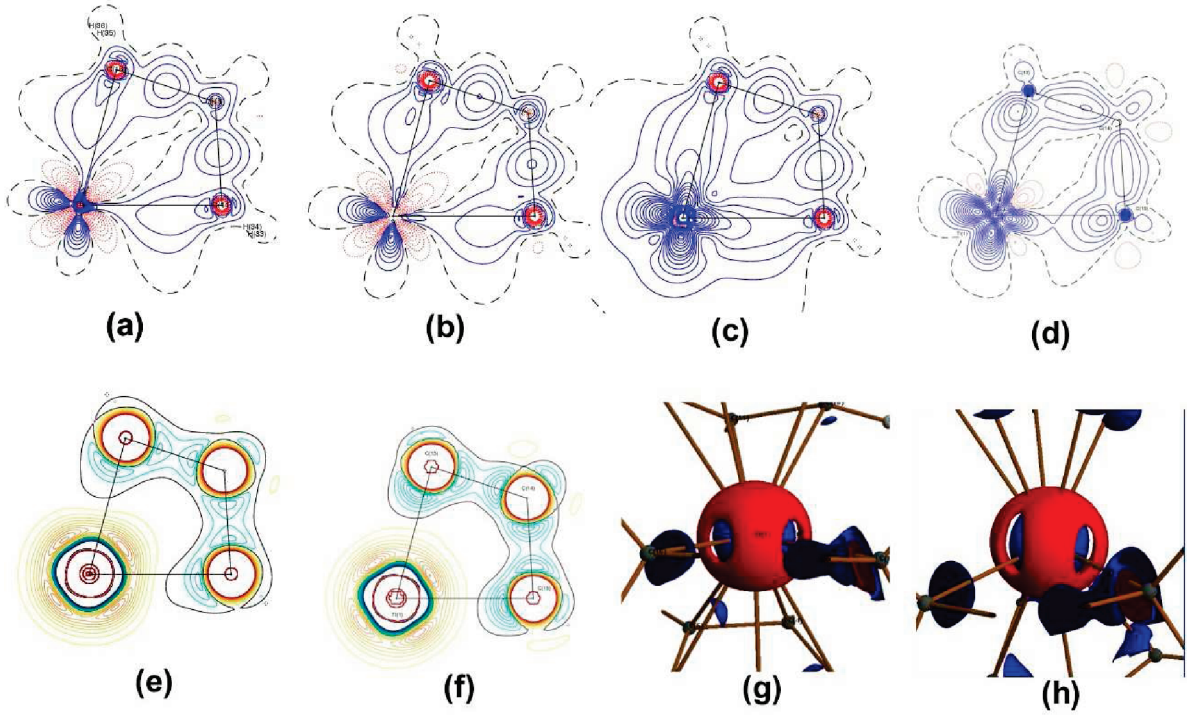

Figure 4. Deformation densities (B3LYP) in the plane containing Ti−C13−C14−C15 (contours at 0.1 e/Å^3, blue/red: negative/positive). (a−c) Theoretical densities: (a) Wachters+f for Ti atom; (b) LanL2DZ for Ti atom; (c) 6-311++G** for Ti atom; (d) experiment; (e) theoretical Laplacian (6-311++G** for Ti atom),(f) experiment; contours at 5 e/Å^5 blue/orange: negative/positive, and 3D representation of the Laplacian around the Ti atom,(g) for theory (6-311++G** for Ti atom) and (h) for experiment; isovalues blue, 5 e/Å^5; red, 37 e/Å^5.

Table 2. Some Features of the Electron Density Distribution of the C−Ti Interaction[a]

bond	bond path length	ρ (e/Å^3)	$\nabla^2\rho$ (e/Å^5)	G (au)	V(au)	H(au)	G/ρ (au)	H/ρ (au)
Ti−C13	2.15	0.523	5.6	0.079	−0.100	−0.021	1.0218	−0.272
		0.655	1.1	0.067	−0.122	−0.0549	0.68835	−0.565
Ti−C15	2.13	0.550	6.1	0.086	−0.109	−0.023	1.0546	−0.282
		0.671	1.3	0.070	−0.127	−0.0568	0.70666	−0.571
Ti−C3	2.38	0.314	4.2	0.046	−0.049	−0.003	0.9948	−0.059
		0.321	3.3	0.041	−0.0473	−0.00652	0.85674	−0.137
Ti−C7	2.44	0.286	3.8	0.041	−0.043	−0.002	0.9691	−0.039
		0.302	3.5	0.040	−0.0444	−0.00416	0.89972	−0.0930
Ti−C8	2.41	0.285	3.8	0.041	−0.043	−0.002	0.9711	−0.037
		0.303	3.9	0.043	−0.0459	−0.00294	0.95727	−0.0654
Ti−C9	2.38	0.291	3.8	0.042	−0.044	−0.002	0.9667	−0.046
		0.323	3.3	0.041	−0.0478	−0.00657	0.86111	−0.137

[a] The first line gives experimental values; the second line gives theoretical values from the calculation with Dobbs and Hehre 6-311G++ basis set for the Ti atom.

As the three theoretical calculations of the title complex gave almost exactly the same values for the bond descriptors, only the 6-311++G** calculations are compared with experiment in Table 2, the full list being given in Table S2 of the Supporting Information. The Kirshnitz approximation[62,63] has been used to derive the experimental value of G(**r**). The values agree well, except for the Ti−C$_\alpha$ bonds. Both methods agree that G(**r**) is larger in the Ti−C$_\alpha$ bonds than in the Ti−C (cyclopentadienyl) critical points. The total energy density for the bonds involving Ti is slightly negative indicating a shared interaction. Nevertheless, the ratio G(**r**)/ρ(**r**) is little higher than 1 (1.021 and 1.054), suggesting that the conclusion of Macchi and Sironi similarly applies to transition metal−carbon bonds. Experimental values of H(**r**)/ρ(**r**) at Ti−C$_\alpha$ BCPs are more negative (−0.272 and −0.282 au) than those at the BCPs of the Ti−cyclopentadienyl bond paths (average value −0.045 au), indicating that the Ti−C13, Ti−C15 interactions have a substantial larger shared character, in agreement with the conclusions of Farrugia et al.[57]

4.3. Electron Density and the Agostic Interaction. Scherer et al. have proposed the ellipticity profile along the bond path of an interacting atom pair as a charge density descriptor for the presence or absence of agostic interactions.[39] Whereas values greater than zero occur in aromatic systems in which the density is distorted from σ-symmetry in the direction of the π-bonds,

(56) Volkov, A.; Abramov, Y.; Coppens, P.; Gatti, C. *Acta Crystallogr.* **2000**, *A56*, 332–339.
(57) Farrugia, L.; Evans, C.; Lentz, D.; Roemer, M. *J. Am. Chem. Soc.* **2009**, *131*, 1251–1268.
(58) Cremer, D.; Kraka, E. *Angew. Chem., Int. Ed.* **1984**, *23*, 627–628.
(59) Bader, R., *Atoms in Molecules. A Quantum Theory*; Oxford University Press: New York, 1994; p 438.
(60) Macchi, P.; Sironi, A. *Coord. Chem. Rev.* **2003**, *238−239*, 383–412.
(61) Gibbs, G. V.; Spackman, M. A.; Jayatilaka, D.; Rosso, K. M.; Cox, D. F. *J. Phys. Chem. A* **2006**, *110*, 12259–12266.
(62) Kirzhnitz, D. A. *Sov. Phys. JETP* **1957**, (5), 64–72.
(63) Abramov, Y. A. *Acta Crystallogr.* **1997**, *A53*, 264–272.

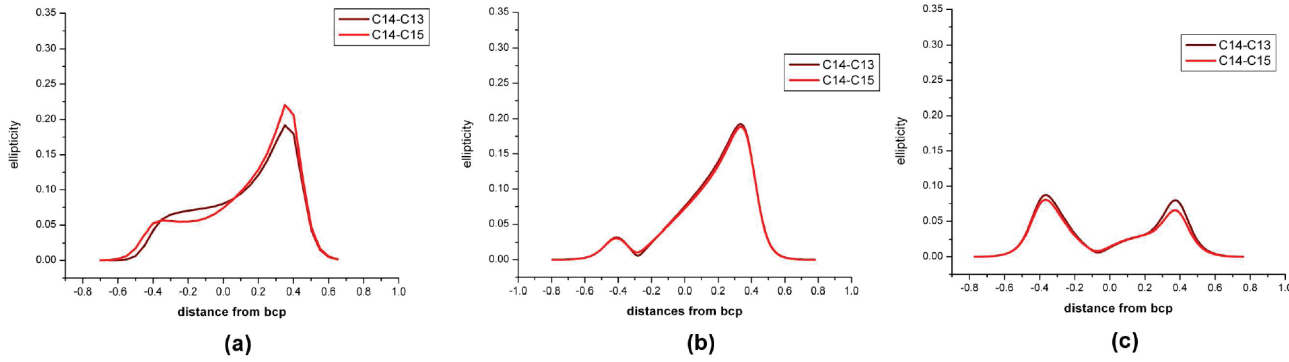

Figure 5. Ellipticity (ε) profile along the $C_\alpha-C_\beta$ bond paths in the neopentadiyl ligand calculated from experimental density, $\varepsilon = \lambda_1/\lambda_2 - 1$. (a) Ellipticity of the experimental density in the C14−C13 and C14−C15 bonds, the largest ellipticity is close to the Ti atoms, (b) theoretical ellipticity profile along the bond paths; (c) the theoretical ellipticity profile along the bond paths of the corresponding bonds of a Mo compound with no agostic interactions.

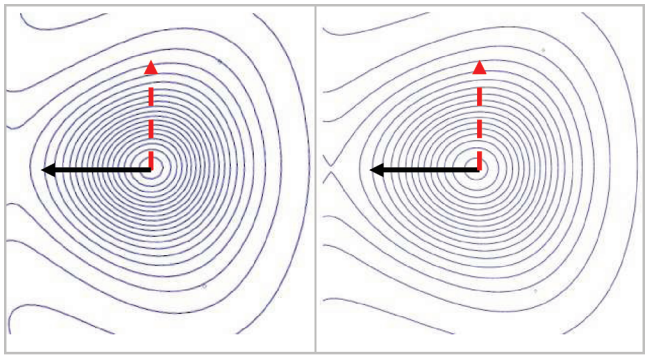

Figure 6. Contour maps of the experimental charge density $\rho(r)$ in the plane perpendicular to the bond path between C14−C15 at ε_{max}. (a) Experiment; (b) theory. Contour interval 0.1 e/Å^3. The orientation of the major distortion axis is indicated by the full arrow (←), which is in the direction of the Ti atom. The broken red arrow is perpendicular to the plane of Ti−C13−C14−C15.

in agostic systems such distortion occurs in the direction of a proximal metal atom. The latter is clearly the case here. The C13−C14 and C15−C14 ellipticity profiles along the bond path show a complex and asymmetric shape in comparison with typical C−C or C═C bonds (Figure 5). These two $C_\alpha-C_\beta$ bonds have considerably larger ellipticities, ε, at their BCPs (0.08/0.07) than the corresponding C−C bonds in the Mo compound (∼0.01) with no agostic interaction,[32] in which the lengthening of the $C_\alpha-C_\beta$ bonds is not observed ($C_\alpha-C_\beta$ 1.528(2) Å). In addition, the curves for the Ti compound in Figure 5a and b show large off-center maxima on the C_α side of the bond (∼0.4 Å from the BCP), giving evidence for the deformation of the

Table 3. Net Atomic Charges on the Ti Atom and the Ligands

	Bader charges	monopole charges	Hirshfeld charges
Ti	+1.12	−0.13	−0.06
$Cp(CH_3)$	−0.45	−0.03	−0.05
	−0.62	−0.18	−0.21
neopentadiyl	−0.05	+0.33	+0.32

$C_\alpha-C_\beta$ bonding density by the electron deficient titanium center. At this point the cross section of the electron density perpendicular to the $C_\alpha-C_\beta$ bond shows a pronounced elongation approximately directed toward the Ti atom (Figure 6a), giving evidence for the presence of the agostic metal C−C bond interaction. The distortion is reproduced in the theoretical density map shown in Figure 6b. These observations strongly support Scherer and McGrady's electron delocalization criterion for the existence of an agostic interaction.

4.4. Net Atomic Charges and d-Orbital Populations. Net experimental charges for the Ti and the ligands are listed in Table 3. As the partitioning of the charge is not uniquely defined three different algorithms have been applied. Results based on Bader's topological AIM theory,[59] from the monopole populations from the XD charge density refinement, and from the Hirshfeld 'stockholder partitioning' of the molecular charge[64] are listed in columns 2−4. The differences between the results are a direct consequence of the different definitions used. The Bader charge on Ti is larger, which may be attributed to the diffuseness of the 4s orbitals, which extend beyond the Ti basin defined by the zero-flux surface of the total density. Nevertheless, all methods agree that space partitioning allocates 3−4 valence electrons to the Ti atom. Similarly, in a charge density

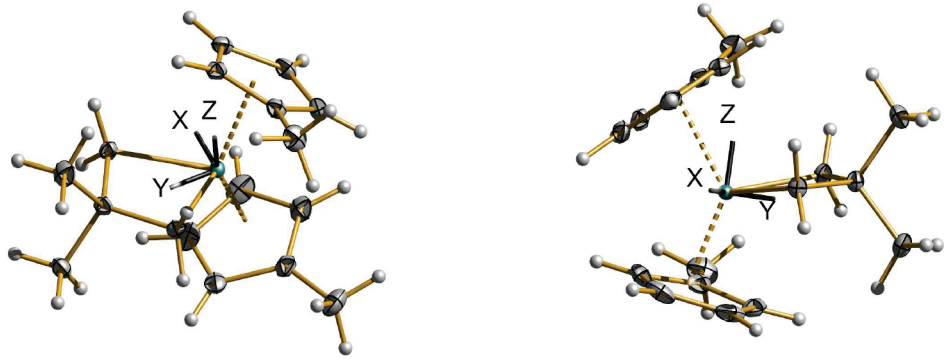

Figure 7. Structure and the coordinate system corresponding to the orientation with minimal $d_{x^2-y^2}$ population on the Ti atom.

Table 4. Percentage Populations of the Ti d Orbitals[a]

	d_{z^2}	d_{xz}	d_{yz}	$d_{x^2-y^2}$	d_{xy}
%	19.4	18.0	16.0	10.0	36.6

[a] The total d-electron monopole population equals 2.13 e.

study of $NH_4[Ti(C_2O_4)_2]\cdot 0.2H_2O$ in which the Ti is formally 3^+, a d-electron population of 1.7−2 electrons was found.[65]

The d-orbital populations can be directly derived from the results of the multipole refinement.[66] For a coordination geometry lacking symmetry the choice of coordinate system can be based on minimizing the population of the cross terms between the density functions, as is done in the program ERD.[67] Figure 7 shows the orientation of the resulting coordinate system, while the corresponding d-orbital population percentages are given in Table 4. The high population of the d_{xy} orbital is in good agreement with the experimental deformation density map (Figure 4d). Populations of the cross terms are listed in Table S3.

5. Conclusions

This experimental electron density study of a 16-electron titanacyclobutane provides direct evidence of the electron density shift expected from the previously proposed presence of (C−C)→Ti agostic interactions. In accord with the model of Scherer and McGrady,[39] the perturbed C−C bonds have significantly greater ellipticities at their bond critical points than the other C−C bonds, and markedly asymmetric maxima in the bond ellipticity on the Cα side of their BCPs. The $C_\alpha-C_\beta$ bond density at these maxima is elongated toward the metal center. Thus, even though there may be rather modest increases in C−C bond lengths as a result of the agostic interaction, an accurate electron density study can provide convincing support for the interaction. That this method can be applied to paramagnetic, thermally sensitive, and/or insoluble compounds indicates that it can be a useful complement or alternative to other methods. Other species have been reported which appear to be candidates for such studies. They include molybdenacyclobutanes with both elongated C−C bonds[68] and characteristically high $J(^{13}C-H)$ values,[69,70] similar tungsten analogues,[71] and ruthenacyclobutanes with low $J(^{13}C-^{13}C)$ and high $J(^{13}C-H)$ values.[72−76] In each case the data point to substantially greater agostic interactions than observed here.

One other point of interest is that despite the formal d^0 electron configuration for this Ti(IV) species, significant electron density nonetheless was found to reside in the d orbitals. This could have significant implications for the chemistry of these species, for example by allowing for backbonding interactions with π acid ligands. The observed nonzero d electron population in the formally d^0 Ti atom again indicates that formal charges do not represent the actual distribution of the electrons in molecular space.

All three theoretical calculations reproduce the observed deformation density in the ligand, but whereas the 6-311++G** basis set for Ti agrees well with the experimental results in the *xy* plane of the Ti atom, this is not the case for the two other basis sets tested in this work.

Acknowledgment. Support of this work by the National Science Foundation (CHE0236317) is gratefully acknowledged.

Supporting Information Available: A full description of ref 47. Table S1 with bond lengths and topological values at the critical points. Table S2 with topological parameters describing the C−Ti interaction. Table S3 with d orbital cross terms for the coordinate orientation described in the text. X-ray crystallographic data for the title compound (CIF). This material is available free of charge via the Internet at http://pubs.acs.org.

JA807649K

(64) Hirshfeld, F. L. *Theor. Chim. Acta* **1977**, *44*, 129–38.
(65) Sheu, H. S.; Wu, J. C.; Wang, Y.; English, R. B. *Acta Crystallogr.* **1996**, *B52*, 458–464.
(66) Holladay, A.; Leung, P. C.; Coppens, P. *Acta Crystallogr.* **1983**, *A39*, 377–387.
(67) Sabino, J. R.; Coppens, P. *Acta Crystallogr.* **2003**, *A59*, 127–131.
(68) Graham, P. M.; Buschhaus, M. S. A.; Pamplin, C. B.; Legzdins, P. *Organometallics* **2008**, *27*, 2840–2851.
(69) The $J(^{13}C-H)$ values for the reported complex 2B are 156, 155, and 136 Hz for C(1,2,6), while for complex 5D the values are 142.5, 139.5, and 133.5 Hz for C(1,2,9).[70]
(70) Graham, P. M.; Legzdins, P.; Turpin, G. C.; Harvey, B. G.; Ernst, R. D., unpublished results.
(71) Buschhaus, M. S. A.; Pamplin, C. B.; Blackmore, I. J.; Legzdins, P. *Organometallics* **2008**, *27*, 4724–4738.
(72) Romero, P. E.; Piers, W. E. *J. Am. Chem. Soc.* **2005**, *127*, 5032–5033.
(73) Romero, P. E.; Piers, W. E. *J. Am. Chem. Soc.* **2007**, *129*, 1698–1704.
(74) van der Eide, E. F.; Romero, P. E.; Piers, W. E. *J. Am. Chem. Soc.* **2008**, *130*, 4485–4491.
(75) Wang, H.; Metzger, J. O. *Organometallics* **2008**, *27*, 2761–2766.
(76) See also Boulho, C.; Keys, T.; Coppel, Y.; Vendier, L.; Etienne, M.; Locati, A.; Bessac, F.; Masseras, F.; Pantazis, D. A.; McGrady, J. E. *Organometallics* **2009**, *28*, 940–943.